SCREW DISLOCATIONS IN GaN GROWN BY DIFFERENT METHODS

Z. Liliental-Weber, D. Zakharov, J. Jasinski, M.A. O'Keefe and H. Morkoc[a]

Lawrence Berkeley National Laboratory, Berkeley, CA 94720 m/s 62/203

[a] Virginia Commonwealth University, Richmond, VA

ABSTRACT

A study of screw dislocations in Hydride-Vapor-Phase-Epitaxy (HVPE) template and Molecular-Beam-Epitaxy (MBE) over-layers was performed using Transmission Electron Microscopy (TEM) in plan-view and in cross-section. It was observed that screw dislocations in the HVPE layers were decorated by small voids arranged along the screw axis. However, no voids were observed along screw dislocations in MBE overlayers. This was true both for MBE samples grown under Ga-lean and Ga-rich conditions. Dislocation core structures have been studied in these samples in the plan-view configuration. These experiments were supported by image simulation using the most recent models. A direct reconstruction of the phase and amplitude of the scattered electron wave from a focal series of high-resolution images was applied. It was shown that the core structures of screw dislocations in the studied materials were filled. The filed dislocation cores in an MBE samples were stoichiometric. However, in HVPE materials, single atomic columns show substantial differences in intensities and might indicate the possibility of higher Ga concentration in the core than in the matrix. A much lower intensity of the atomic column at the tip of the void was observed. This might suggest presence of lighter elements, such as oxygen, responsible for their formation.

INTRODUCTION

Thin film heteroepitaxy of polar materials such as GaN grown by Metal-Oxide-Chemical-Vapor-Deposition (MOCVD), Molecular-Beam-Epitaxy (MBE) or Hydride-Vapor-Phase-Epitaxy (HVPE) on SiC or Al_2O_3 is hampered by the formation of structural defects, primarily dislocations. The typical density of threading dislocations in (0001) GaN grown on Al_2O_3 is in the range of 10^9-10^{11} cm^{-2}. These dislocations propagate vertically from the GaN/Al_2O_3 interface to the GaN surface (Heying et al., 1996; Ponce et al., 1996).

Nanotubes and pinholes are other types of defects present in this material (Liliental-Weber et al., 1997a;1997b) These defects are empty areas, which either extend along the growth direction (tubes) or form V-shape defects on (10$\underline{1}$1) planes with hexagonal shaped bases along the c-plane. In most cases nanotubes and pinholes are formed close to the dislocations, but in some cases these defects are formed in dislocation free areas. The density of these defects was estimated to be in the range of 10^5 -10^7 cm^{-2} and their radii in the range 3–1500 nm. It was suggested (Liliental-Weber et al., 1997a;1997b) that these two types of defects are related to the presence of impurities in the material, supporting theoretical work by Elsner et al., (1998) who showed that O and O-related defect complexes can be formed on the walls of nanopipes in GaN. Cherns et al., (2000) suggested that nanopipes form under non-equilibrium conditions and are influenced by growth factors.

Despite this high density of dislocations (and other defects), a high emission efficiency has been achieved in optical devices such as light-emitting diodes (LEDs) and laser diodes (LDs) (Nakamura et al., 1998). This behavior may be contrasted with that of GaAs-based LDs where a value of dislocation density of about 10^4 cm^{-2} is usually sufficient to prevent laser action (Lester et al.,1995). The most common explanation for this phenomenon is that the threading

dislocations in GaN do not have electronic states in the band gap. However, this is still a controversial issue, and there is no agreement on this subject between different scientific groups (Elsner et al.,1997, Elsner et al.,1998, Keller et al., 1996, Wright et al.,1998).

There are also discrepancies concerning the nature of dislocation cores in GaN. Some investigators claim that GaN dislocations have open cores (Qian et al.,1995) but others suggest that screw dislocations have full cores (Arslan & Browning, 2002). First-principles total energy calculations showed Ga-filled screw dislocation cores to be stable in Ga-rich growth conditions (Northrup, 2001 & 2002). Scanning current-voltage microscopy (SIVM) studies showed that leakage occured at screw/mixed dislocations but not at pure edge dislocations (Hsu et al., 2001). These authors concluded that the reverse bias current in GaN was carried by dislocations with a screw component, with Ga accumulated at or near screw dislocations and that Ga affects the dislocation electrical activity.

The aim of this work was to find if screw dislocations have full or empty cores and to determine the core stoichiometry in the case of a full core.

EXPERIMENTAL

Two sets of samples were grown by two different growth methods: HVPE and MBE. MBE samples were grown using Ga rich and Ga-lean conditions using HVPE templates, as in earlier experiments (Hsu et al., 2001). Transmission Electron Microscopy (TEM) has been applied to study these layers in electron-transparent samples in plan-view and in cross-section. Determination of dislocation core structure from plan-view samples was carried out using a modified 300keV field emission Philips electron microscope (OÅM-CM300) to obtain high-resolution focal series with a constant defocus step. The electron exit wave from the crystal

structure was obtained by numerical reconstruction (Thust et al., 1996) from the full focal series of 20 images. The models proposed for screw dislocations (Northrup, 2002) for stoichiometic (6:6 model) and Ga rich (6:0 model with N atoms removed from the dislocation core allowing Ga-Ga bondings along the helix) model were used for image calculations expected in the electron microscope for specific sample thickness and defocus and also to simulate focal series reconstruction. In addition, the exit surface wave was calculated for GaN where some N-atoms were substituted by Ga-atoms within one atomic column, to observe the image change for heavier than matrix column of atoms.

Screw dislocations have displacements along the c-axis, therefore, continuous tilt of c-planes is observed (Figs. 1a, b). For this reason one would need to know how this tilt affects the experimental images. In order to learn how the image is changing with the sample tilt and with change of stoichiometry the focal series were simulated using Mac Tempas programs (O'Keefe & Kilaas, 1987). The Thust program (Thust et al., 1996) was then applied to obtain numerical phase and amplitude reconstruction at the sample exit plane.

RESULTS OF IMAGE SIMULATION

Image simulation (Fig. 2a) using Mac Tempas programs for pure GaN in the range of sample thickness 20Å to 320Å shows that already at 80Å, the phase of the exit-surface wave changes from white atoms to black atoms. This is an effect of an interaction between primary and diffracted beams, which changes with sample thickness, tilt and sample composition. To obtain useful information, the sample thickness need to be chosen in such a way that all beams contributing to image formation have similar phases and do not attenuate each other. The black atom image changes again at the sample thickness of 160Å where a white-atoms image is present

up to 220Å before changing to black atoms again. At the sample thickness of 320Å the image once again resembles the image at 20Å thickness. In each case the image has six fold symmetry.

The situation changes with specimen tilt. For a 4 mrad tilt along 0001 axis, a partial change from white atoms to black atoms starts already at the thickness of 60Å. The image changes again to white atoms at the sample thickness of 140Å (Fig. 2b). For thin samples like 20Å or 40Å the image still preserves six-fold symmetry. This, however, changes to two-fold for larger sample thickness. If one chooses, for example, the 160Å thick sample then one can observe that pattern symmetry is changing (Fig. 3a,b) and the atomic columns are no longer round (Fig. 3b), as was observed for non-tilted samples (Fig. 3a). One can conclude from these calculations that sample tilt is easy to recognize and then can be taken into account for experimental image interpretation. For samples without tilt, each atomic column has the same intensity, and measurements along specific crystallographic directions (as shown on Fig. 3a) shows the same height (Fig. 3c). However, for small tilts like 4 mrad, due to the symmetry change, tracings along the same crystallographic direction show that the intensity changes by 4.5% (Fig. 3d).

Calculation of an exit surface wave for the 6:6 (Northrup, 2002) stoichiometric dislocation core for small sample thickness like 40Å or 45Å shows that the intensity of all columns remains the same, and it is actually not easy to recognize where the core is present. The only feature which distinguishes the presence of a screw dislocation is a slightly larger channel between atomic columns along the dislocation core, as observed from the calculation of the exit surface wave (Fig. 4a). This larger channel can be also observed in the reconstructed phase images (Fig. 4b) where the channel between atomic columns along the dislocation core has slightly darker contrast, however is hardly visible in the amplitude image (Fig. 4c). These exit-

surface-wave images (Fig. 4d), reconstructed for phase (Fig. 4e) or amplitude (Fig. 4f) do not change after sample was tilted by 4 mrad.

Calculation of an exit surface wave for the 6:0 Ga-rich dislocation core shows a difference in intensity of the atomic columns along the core compared to the intensity of the matrix columns. Similar information can be obtained from the reconstructed phase image (Fig. 5). In the phase image one can notice that the matrix and the Ga-rich dislocation core (formed by removing N-atoms from the core) behave differently. It is only for small sample thicknesses (40 and 45Å) that both have white atomic columns (Fig. 5a), while already for a sample thickness of 60Å, the matrix columns start to change to black, while the core still remains white (Fig. 5b). This occurs because the dislocation core columns are lighter, since in this model all N-atoms were removed making these columns lighter than the matrix. Slight changes to the black atoms along the dislocation core start to appear at a thickness of 140Å (Fig. 5c). At a thickness of 350Å atomic columns in both the matrix and the dislocation core atomic columns have black atoms but with distinguishable intensity (Fig. 5d). Due to the delayed change from white atoms to black atoms between the matrix and the core, and the strong intensity change for the same color of atoms, a Ga-rich intensity core should be easy to recognize for any sample thickness. This information still remains valid even if a small sample tilt is introduced. The strong intensity difference between the matrix and the core is preserved.

If an atomic column is heavier than a matrix column, then this column will have much brighter intensity than the matrix columns for thin sample (40Å), and this intensity will increase with the change of Ga occupancy for the same sample thickness (Fig. 6 a-c). However if the sample thickness is larger (80Å), then this heavier atomic column will change to the black atom image much faster than the matrix (Fig. 6 d-f).

EXPERIMENTAL RESULTS AND DISCUSSION

TEM studies of the MBE samples grown under Ga excess conditions in plan-view and in cross-section samples showed that the sample surface was covered by small Ga droplets (Fig. 7 a,b) . Some of these droplets could be found inside the layer (Fig. 7b). Screw dislocations could be found in these samples but only in some rare cases were Ga droplets located on top of them, as similarly described earlier (Hsu et al., 2001). One needs to emphasize that Ga droplets have always a round shape (marked by arrows on Fig. 7a,b); therefore it was easy to distinguish them from other inhomogeneities on the sample surface or inside the layer.

TEM studies of the HVPE samples in cross-section showed the presence of small voids along the screw dislocation lines (Fig. 8a,b). This was easy to observe under **g.b**=0 diffraction conditions, for which screw dislocations are out of contrast (10b and d). These voids were not observed for edge dislocations in the same material and not at all in the MBE overlayer samples grown on top of the HVPE template (see Fig. 7 a,b). It was also noticed that these voids were observed in the HVPE layer obtained from different crystal growers (Fig. 8c and d). However, when MOCVD layers were grown on top of the HVPE template voids were not observed in this part of the sample (Fig. 8d), similar to MBE grown samples.

In order to obtain information about dislocation core structures, observations were performed in the plan-view configuration. No displacement vector can be observed around screw dislocations in plan-view configuration, as expected for screw dislocations since the displacement vector is along the c-axis. Figures 9a,b show that indeed this applies for dislocations in both HVPE and MBE samples. When a high-resolution image is taken at Scherzer defocus, it can be seen that only part of the image has an on-axis orientation (Fig. 9a-right hand

side). The remaining part of the image has some tilt, which is caused by the tilted c-lattice planes surrounding the screw dislocation (compare with the model presented in Fig.1). This explains why it was necessary to calculate expected reconstructed phase and amplitude images and how they change with tilt.

As expected from the cross-sectioned samples, voids are observed surrounding dislocations in the HVPE sample. These voids have a hexagonal shape (lighter contrast in the central part of Fig. 9b). To obtain structural information at higher resolution, 20 micrographs were obtained from each screw dislocation at large values of defocus and the complex electron wave was reconstructed numerically (Thust et al., 1996). An image of the phase of the exit-surface wave gives information on the distribution of atomic columns. Usually additional micrographs were taken at Scherzer defocus before the series of 20 images and after, to check on image drift during this long exposure time. Only low-drift images were taken for phase and amplitude reconstruction procedure and then further interpreted.

In order to learn if a dislocation has full or open core, we looked for missing atomic columns expected for the empty core as predicted theoretically (Elsner et al.,1997) as shown in Figure 10a. We were also looking for changes in intensity of particular columns or any indication of change from white to black atomic columns which would be expected for a nonstoichiometric core at the particular sample thickness and sample tilt.

The focal-series reconstruction technique described above was applied to Ga-rich MBE grown samples in [0001] projection where atomic columns are separated by 1.84Å. Fig. 10b shows the core structure of a Ga-rich sample. One can notice that the image is tilted and the channel between atomic column is not in the center, therefore the whole image has two–fold symmetry, as expected from our earlier calculations (see Fig. 2). However, no change in intensity

between particular atomic columns can be observed for the atomic columns in the center of this image and on the sides, indicating that atomic columns at the dislocation core and outside have similar stoichiometry. An expected, slightly larger channel between the atomic columns was also not observed, most probably due to some noise expected for the experimental image. Similar information was obtained for the Ga-lean samples (Fig. 10c). This image is much less tilted than the previous one and it is possible to notice the c-plane tilt as expected from the model of screw dislocation (Fig.1). However, no expected change in the intensity of particular atomic column in the center of the image compared to the outside areas is observed, suggesting that the dislocation cores studied in these samples were stoichiometric. However, these images, obtained for both Ga-rich and Ga-lean samples, show no clear gap as would be expected for the open dislocation core, therefore in both these cases dislocations have full core. This result is in agreement with early work (Arslan et al., 2002).

Similar focal-series reconstructions were obtained for [0001] projections of screw dislocations accompanied by voids in HVPE samples (Fig. 11a). Since the void surrounds the dislocation it would be expected that perhaps such a dislocation has an open core. Examination of the intensity of particular columns does not allow us to come to such a conclusion, since all six columns in each cell are present, but their intensity differs. Therefore, even in the sample where a screw dislocation is decorated by voids, a screw dislocation has a full core. In the dislocation core area, one atomic column appears to be very weak (Fig. 11a) and in the magnified core image shown in Fig. 11b- (column circled in the upper-left corner) there is another column which is very bright (Fig. 11b- column circled in the center). These columns are not adjacent to one other, but separated by 8 Å. This distance is comparable to that between a dislocation line and the tip of the pyramidal voids observed in cross-section samples. The

intensities of the highest-intensity and lowest-intensity atomic columns lie more than three standard deviations from the mean atomic column peak intensity in the matrix (Fig. 11c). Therefore, the intensity difference between the highest-intensity and lowest-intensity atomic columns is about six standard deviations. The observed change in intensity between the highest-intensity and lowest-intensity atomic columns cannot be obtained simply by sample tilt, therefore this difference in their intensity can be assigned only to the stoichiometry of the particular columns. It also does not appear that this large intensity fluctuation (6 standard deviations) could be an artifact of electron beam damage, since such fluctuations were not observed in the matrix or at the dislocation cores in the samples grown by MBE. One can also notice that the intensity of one column within the core is much brighter than intensities of other columns which would suggest that this column is heavier than matrix. As described above in this model (Northrup, 2002) N was removed from the particular columns introducing "N-like vacancy" and expected intensities of such columns were always lower. Our experiment would suggest that some N atoms were substituted by Ga and N-vacancies were not introduced.

The column with the lowest intensity can be attributed to the tip of the void since the small sample thickness and possibility of the light atom responsible for the void formation would be expected. This would be in agreement with our earlier suggestion that light elements such as oxides are responsible for the formation of pinholes (voids) and empty nanotubes (Liliental-Weber et al., 1997a). The highest intensity column with the significant change of intensity could be assigned to the stoichiometry change and the excess and possibility of higher concentration of Ga atoms. Based on comparison with cross-section images, it is clear that the location of the tip of the void does not need to overlap with a dislocation line, but the intensity difference with the surrounding matrix suggests that the dislocation core might have more Ga atoms (Northrup,

2001). It is possible that not only strain at dislocations, but also an excess of Ga within the core, may attract impurities (light elements), giving the reason for formation of voids close to the dislocation line.

CONCLUSIONS

Image simulations were performed for screw dislocations with different core stoichiometries. Two different models proposed by Northrup were calculated: stoichiometric 6:6 and Ga-rich 6:0 (Northrup 2001 & 2002). The effect of substitution of N by Ga atoms was also calculated. For each model change in sample thickness and sample tilt was also calculated. This was necessary for better understanding of continuous tilt of c-planes around screw dislocation since a displacement vector is along c-axis. High-resolution reconstructions of the phase and amplitude of the complex electron exit wave scattered from HVPE and MBE grown sample were carried out using focal series consisting of 20 under-focused images. The reconstructed phase images showed that screw dislocations in GaN grown by these two methods are different. The main difference appears in the formation of voids with pyramidal shape stacked on top of each other along a dislocation line in the samples grown by HVPE. These voids are never observed in MBE grown material, even when MBE samples were grown directly on HVPE substrates. They were never observed along edge dislocations. All observed screw dislocations had full cores independent of the growth method. In MBE grown materials dislocation cores appear to be stoichiometric. However, in the HVPE grown material some high intensity columns were observed within the dislocation core suggesting a possibility of stoichiometry change and a presence of higher concentration of Ga atoms along some atomic columns within the dislocation core. It is speculated that Ga-rich atomic columns along screw dislocations can attract impurities

present in the sample. From comparison between the samples grown by different methods it confirms the expectation that MBE method is much cleaner in comparison to the HVPE grown samples.

ACKNOWLEDGEMENT

Work supported by the U.S. Department of Energy under contract DE-AC03-76SF00098. The authors would like to express our gratitude to Dr. J. Northrup for sharing his models for screw dislocations with different stoichiometry. Use of the OAM facility at the National Center for Electron Microscopy at the LBNL is greatly appreciated.

REFERENCES:

ARSLAN, I., & BROWNING, N.D. (2002). Intrinsic electronic structure of threading dislocations in GaN. *Phys Rev B* **65**, 075310.

CHERNS, D. (2000). The structure and optoelectronic properties of dislocations in GaN. *J Phys Condens Matter* **12**, 10205.

ELSNER, J., JONES, R., SITCH, P. K., POREZAG, V. D., ELSTNER, M., FRAUENHEIM, TH., HEGGIE, M. I., ÖBERG, S., &. BRIDDON, P. R. (1997). Theory of threading edge and screw dislocations in GaN. *Phys Rev Lett* **79**, 3672.

ELSNER, J., JONES, R., HAUGK, M., GUTIERREZ, R., FRAUENHEIM, TH., HEGGIE, M. ÖBERG, S., & BRIDDON, P. R., (1998). Effect of oxygen on the growth of (1010) GaN surfaces: The formation of nanopipes. *Appl Phys Lett* **73**, 3530.

HEYING,B,. WU, X. H., KELLER, S. , LI, Y., KAPOLNEK, D., KELLER, B. P., DENBAARS, S. P., & SPECK, J. (1996). Role of threading dislocation structure on the x-ray diffraction peak widths in epitaxial GaN films. *Appl Phys Lett* **68**, 643.

HSU, J.W.P., MANFRA, M.J., CHU, S.N.G., CHEN, C.H., PFEIFFER, L.N.,& MOLNAR, R.J. (2001). Effect of growth stoichiometry on electrical activity of screw dislocations in GaN films grown by molecular-beam epitaxy. *Appl Phys Lett* **78**, 3980.

KELLER, S., KELLER, B. P., WU, Y-F., HEYING, B., KAPOLNEK, D., SPECK, J. S., MISHRA, U. K., & DENBAARS, S. P. (1996). Influence of sapphire nitridation on properties of gallium nitride grown by metalorganic chemical vapor deposition. *Appl Phys Lett* **68**, 1525.

LESTER, S.D., PONCE, F. A., CRAFORD, M.G., & STEIGEWALD, D.A. (1995). High dislocation densities in high efficiency GaN-based light-emitting diodes. *Appl Phys Lett* **66**, 1249.

LILIENTAL-WEBER, Z., CHEN, Y., RUVIMOV, S., & WASHBURN, J. (1997a). Formation Mechanism of Nanotubes in GaN. *Phys Rev Lett* **79**, 2835.

LILIENTAL-WEBER, Z., WASHBURN, J., PAKULA, K., & BARANOWSKI, J. (1997b). Convergent Beam Electron Diffraction and Transmission Electron Microscopy Study of Interfacial Defects in GaN Homoepitaxial Films. *Microscopy and Microanalysis the J. Electr. Microsc. Soc. Am*. **3**, 436.

O'KEEFE, M.A. & KILAAS, R. (1987). Advances in high-resolution image simulation. *Proc. 6th Pfefferkorn Conf. on Image and Signal Processing*, Niagara Falls, Ontario. Published as Scanning Microscopy suppl. 2 (1988) 225-244.

NAKAMURA, S., SENOH, M., NAGAHAMA, S., IWASA, N., YAMADA, T., MATSUSHITA, T., KIYOKU, H., SUGIMOTO, Y., KOZAKI, T., UMEMOTO, H., SANO, M., & CHOCHO, K. (1998). InGaN/GaN/AlGaN-based laser diodes with modulation-doped

strained-layer superlattices grown on an epitaxially laterally overgrown GaN substrate. *Appl Phys Lett* **72**, 211.

NORTHRUP, J.E. (2001). Screw dislocations in GaN: The Ga-filled core model. *Appl Phys Lett* **78**, 2288.

NORTHRUP, J.E. (2002). Theory of intrinsic and H-passivated screw dislocations in GaN. *Phys Rev* **B 66**, 045204

PONCE, F. A., CHERNS, D., YOUNG, W. T., & STEEDS, J. W. (1996). Characterization of dislocations in GaN by transmission electron diffraction and microscopy techniques. *Appl Phys Lett* **69**, 770.

QIAN, W., ROHRER, G. S., SKOWRONSKI, M., DOVERSPIKE, K., ROWLAND, L. B., & GASKILL, D. K. (1995). Open-core screw dislocations in GaN epilayers observed by scanning force microscopy and high-resolution transmission electron microscopy. *Appl Phys Lett* **67**, 2284.

THUST, A., COENE, W.M.J., OP DE BEECK, M., VAN DYCK, D. (1996). Focal-series reconstruction in HRTEM: simulation studies on non-periodic objects. *Ultramicroscopy* **64**, 211.

WRIGHT, A. F., & FURTHMULLER, J. (1998). Theoretical investigation of edge dislocations in AlN. *Appl Phys Lett* **72**, 3467.

Figure Captions:

Fig. 1. (a) A model of screw dislocations showing displacement "b" along c-axis (A-B); (b) atomic model of screw dislocation seen from the side showing continuous c-plane bending on both sides of the dislocation.

Fig. 2 (a) Image simulation of GaN for different sample thicknesses: 20Å,80Å, 140Å, 200Å, 260Å and 320Å. Note change from white atom image to the black atom image for different sample thickness. (b) Image simulation for the same sample thicknesses with 4 mrad tilt

Fig. 3. (a) and (b) Image simulation for the sample 160Å thick –without tilt and with 4 mrad tilt, respectively. Note symmetry pattern change from six-fold to two fold, a channel between the atomic columns is not longer in the center. (c) and (d) Intensities of atomic columns along (11$\underline{2}$0) plane for the samples shown in (a) and (b). Note atomic column intensity change with the tilt.

Fig. 4. (a) Calculated exit surface wave for the stoichiometric dislocation core model 6:6 without the sample tilt for the sample thickness of 45Å, reconstructed phase (b), and amplitude (c). The effect of tilt by 4 mrad for the same model and same thickness: (d) exit surface wave, (e) reconstructed phase and (f) reconstructed amplitude.

Fig. 5. Reconstructed phase for the calculated Ga-rich dislocation core model 6:0 for which N atoms were removed. Calculations were done for different sample thickness without the sample tilt and (a) shows 45Å thick sample, (b) 60Å , (c) 140Å, and (d) 320Å. Note delayed change for

the dislocation core from white to black atoms. Due to this difference in the contrast the core should be visible practically for each sample thickness.

Fig. 6. Calculated contrast for 40Å sample thickness where Ga occupancy was changed. In this case some N-atoms were replaced by Ga. Note intensity change (brighter columns) with an increase of Ga occupancy: (a-c) 1/6; 1/4; 1/2 respectively. Same occupancy for the sample thickness of 80Å (d-f). Note change to black atoms for the columns here N was substituted by Ga. The change from white atoms to black occurs sooner for heavier Ga occupancy.

Fig. 7. Cross-section of Ga-rich GaN sample grown under Ga-droplet regime. Two areas of the sample are shown taken for two perpendicular diffraction conditions. Ga droplets are indicated by arrows. In (a) droplets are observed on the sample surface. Note their round shape and location of one droplet between edge dislocation (e) and screw dislocation (s). The screw dislocation is out of contrast for this diffraction condition. There were no dislocations under a second droplet. In (b) Ga droplet (a black round dot) is at some distance from the screw dislocation. There were no Ga droplets near other screw dislocations. Under this diffraction condition all screw dislocations were in contrast.

Fig. 8. Cross-section images show screw dislocations in HVPE-grown material; (a)- dislocation in contrast for **g**=(0002) and (b)-out of contrast for **g**=(11$\underline{2}$0)). Note voids stacked vertically. Screw dislocations in the MBE overlayer sample grown on top of the HVPE material (c,d). The arrows indicate the area near the interface between the HVPE template and the MOCVD

overlayer. Note voids along screw dislocation in the HVPE material and lack of them in the MOCVD material.

Fig. 9. Plan view images of screw dislocations in MBE (a) and HVPE (b) GaN. Burgers circuits have no displacement, as expected. Note tilted c-planes around dislocation in (a) and void in (b).

Fig. 10. (a) Model of open core screw dislocation (after Elsner et al., 1997). (b) Full core of screw dislocation in Ga-rich MBE grown GaN and (c) in the Ga-lean GaN. Lack of difference in atomic column intensity between center image and surrounding matrix indicates stoichiometric cores.

Fig. 11. (a) Image reconstruction of screw dislocation in HVPE sample. (b) Magnified image of the dislocation core area. Note (circled) atomic columns with different brightness. Intensity profiles show reduced (A) and enhanced (B) image intensity, indicating Ga excess and deficiency (c).

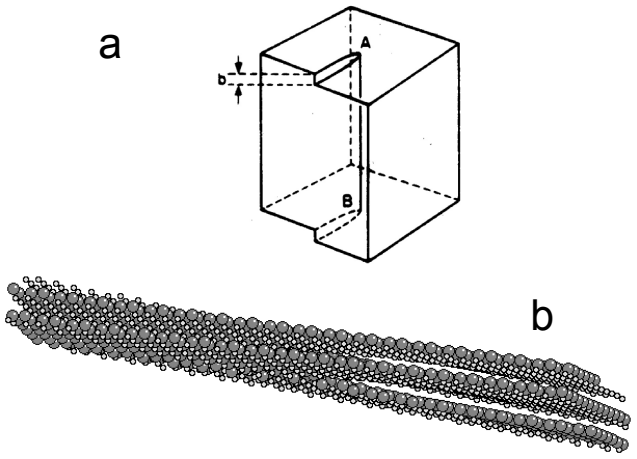

Fig. 1.

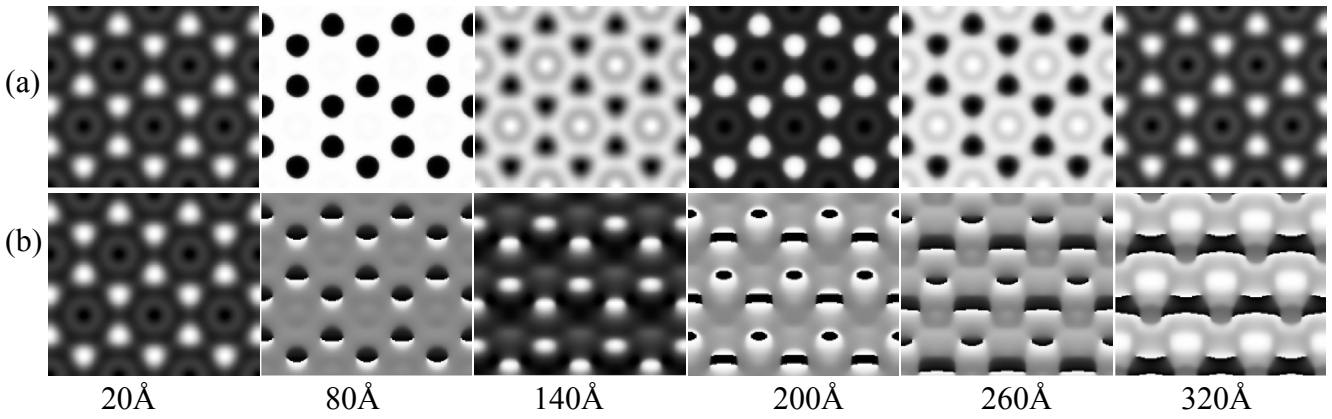

Fig. 2.

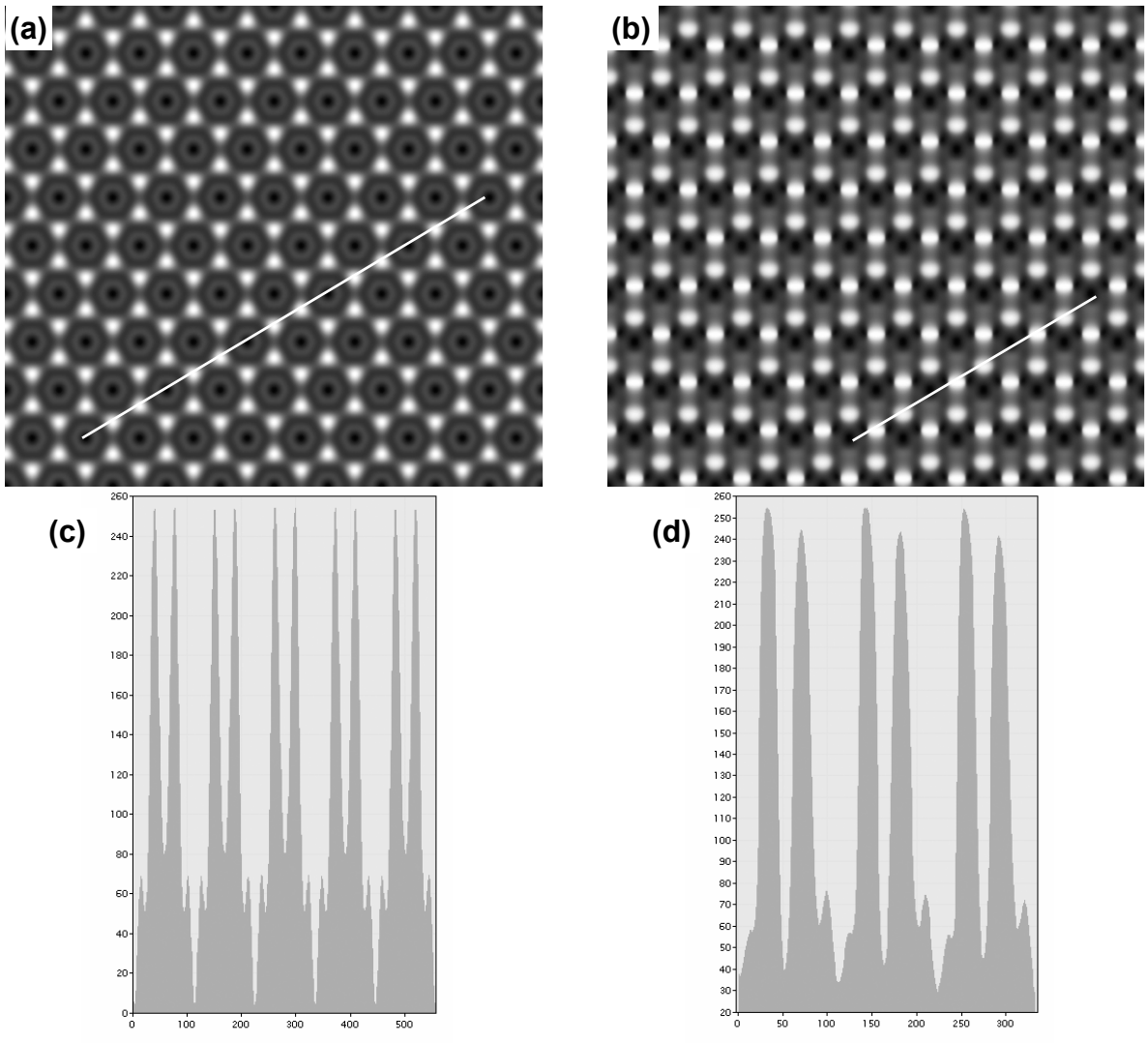

Fig. 3.

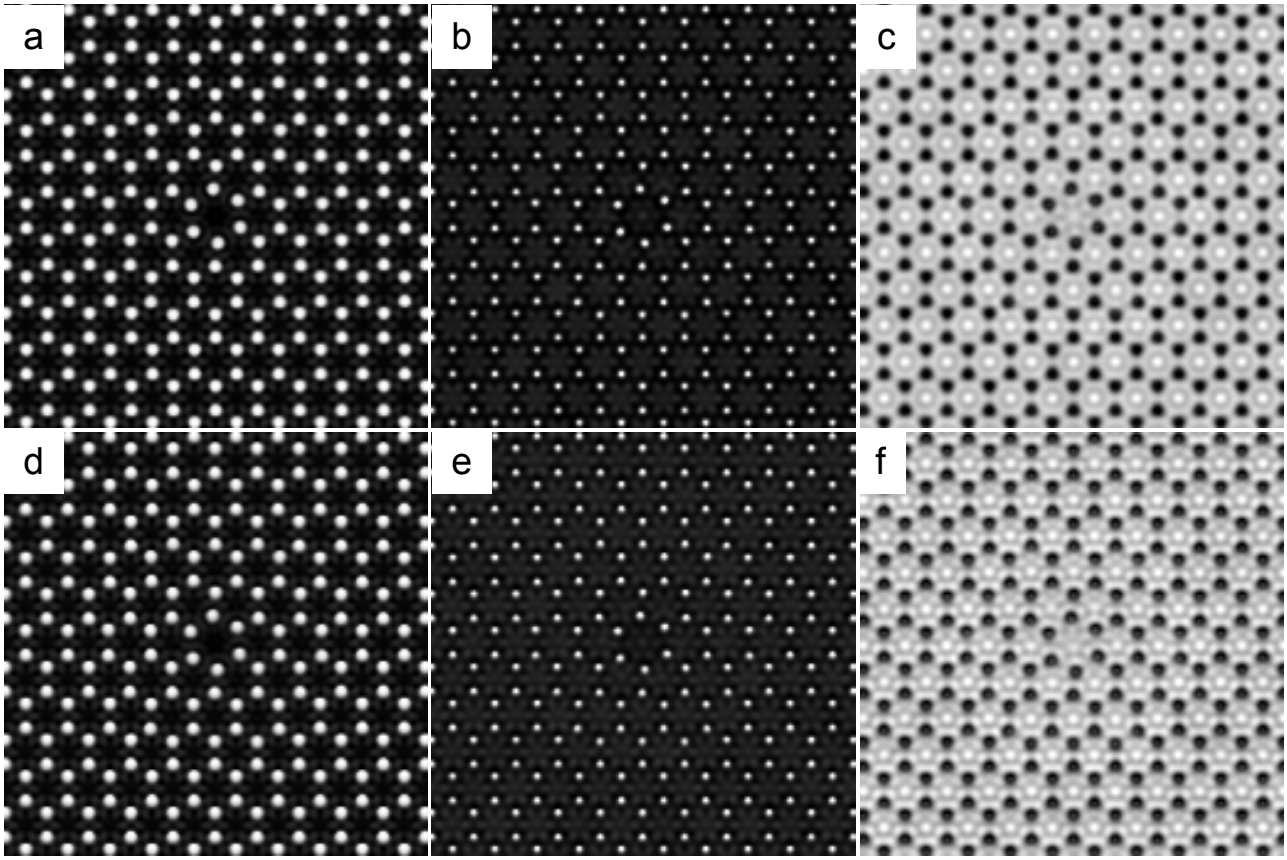

Fig. 4.

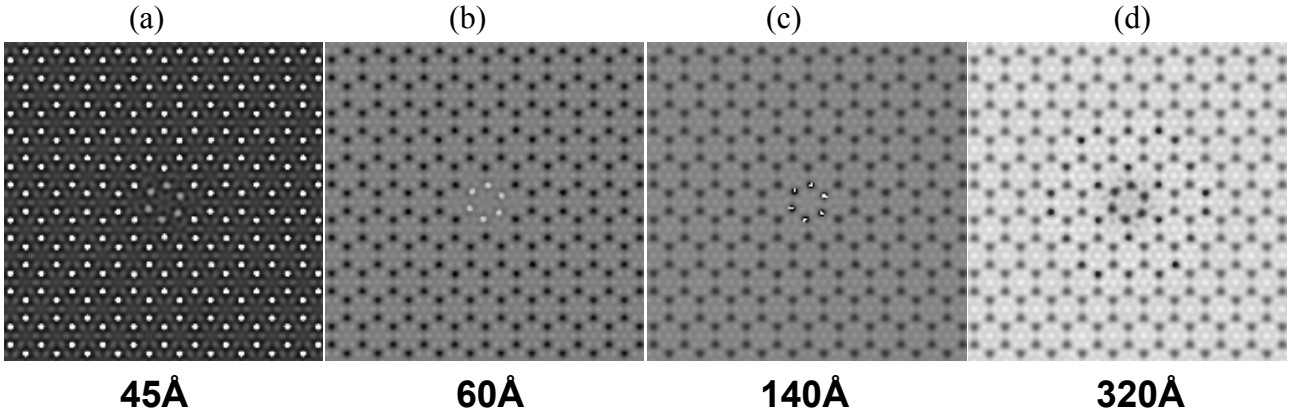

Fig. 5.

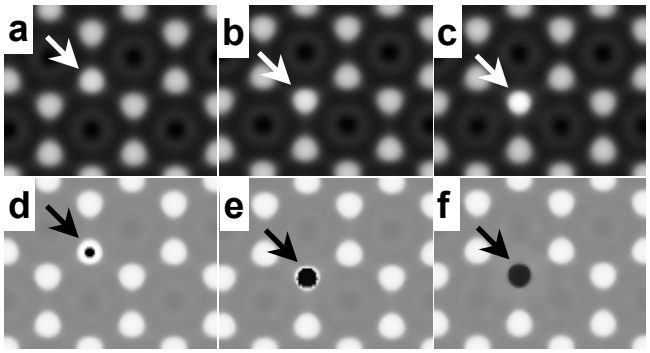

Fig. 6.

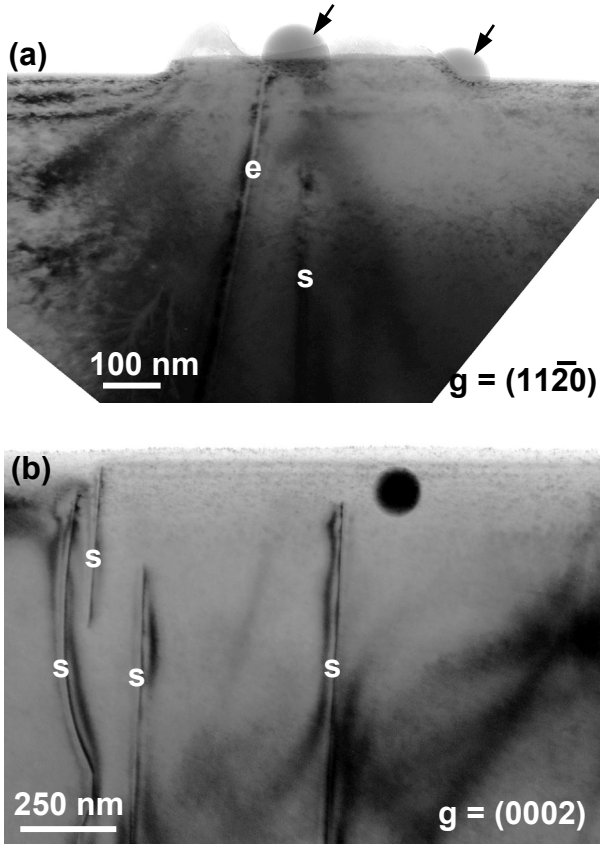

Fig.. 7.

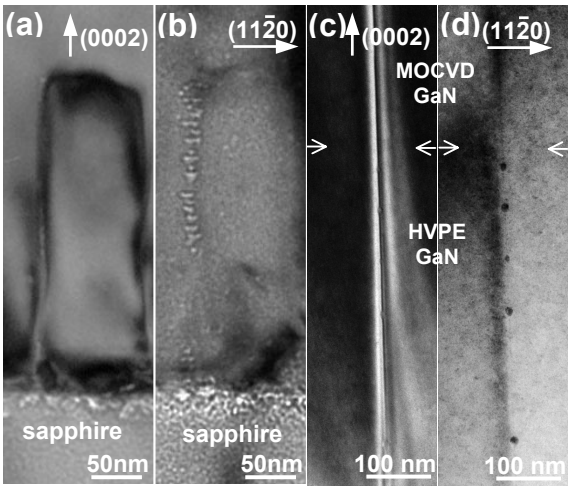
(a)
(0002)
(b)
(11$\bar{2}$0)
(c)
(0002)
MOCVD
GaN
HVPE
GaN
(d)
(11$\bar{2}$0)
sapphire
50nm
sapphire
50nm
100 nm
100 nm

Fig. 8.

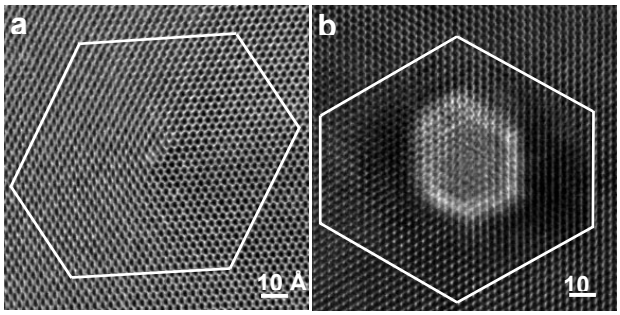

Fig. 9.

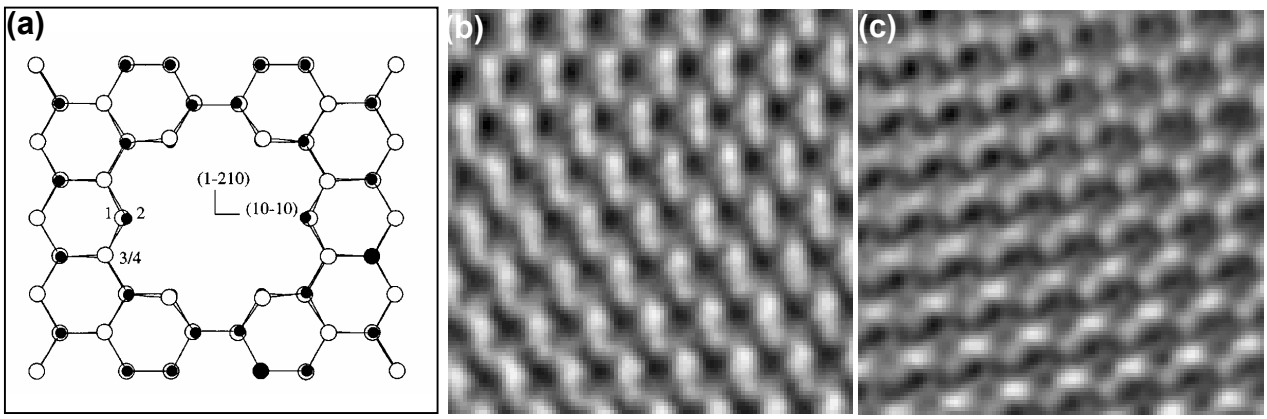

Fig. 10.

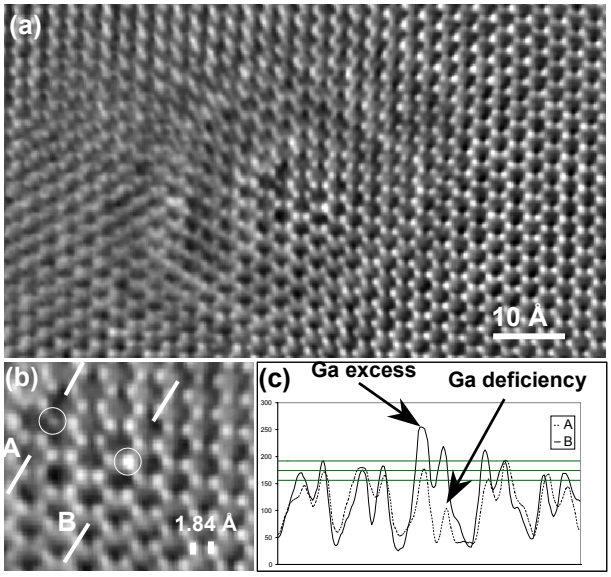

Fig. 11.